IOP Publishing Journal of Physics D: Applied Physics
J. Phys. D: Appl. Phys. **40** (2007) 6631–6640 doi:10.1088/0022-3727/40/21/023

Rf discharge dissociative mode in NF_3 and SiH_4

V Lisovskiy[1], J-P Booth[2], K Landry[3], D Douai[4], V Cassagne[5] and V Yegorenkov[6]

[1] Department of Physics and Technology, Kharkov National University, Kharkov 61077, Ukraine
[2] Laboratoire de Physique et Technologie des Plasmas, Ecole Polytechnique, Palaiseau 91128, France
[3] Unaxis Displays Division France SAS, 5, Rue Leon Blum, Palaiseau 91120, France
[4] Association Euratom-CEA, Département de Recherches sur la Fusion Contrôlée, CEA Cadarache, F-13108 Saint Paul lez Durance Cedex, France
[5] Riber, 31 rue Casimir Périer, 95873 Bezons, France
[6] Department of Physics, Kharkov National University, Kharkov 61077, Ukraine

E-mail: lisovskiy@yahoo.com

Received 11 April 2007, in final form 11 August 2007
Published 19 October 2007
Online at stacks.iop.org/JPhysD/40/6631

Abstract
This paper shows that the rf capacitive discharge in NF_3 and SiH_4 can burn in three possible modes: weak-current α-mode, strong-current γ-mode and dissociative δ -mode. This new dissociative δ-mode is characterized by a high dissociation degree of gas molecules (actually up to 100% in NF_3 and up to 70% in SiH_4), higher resistivity and a large discharge current. On increasing rf voltage first we may observe a weak-current α-mode (at low NF_3 pressure the α-mode is absent). At rather high rf voltage when a sufficiently large number of high energy electrons appear in the discharge, an intense dissociation of gas molecules via electron impact begins, and the discharge experiences a transition to the dissociative δ-mode. The dissociation products of NF_3 and SiH_4 molecules possess lower ionization potentials, and they form an easily ionized admixture to the main gas. At higher rf voltages when near-electrode sheaths are broken down, the discharge experiences a transition to the strong-current γ -mode.

1. Introduction

Rf discharge in NF_3 is widely used for cleaning technological chambers [1–6], etching silicon-containing materials [7–16] and plasma treatment of polymeric dielectrics [17]. This gas is of interest due to the following reasons. The CF_4, C_2F_6, SF_6 gases usually employed for etching semiconductor materials have a number of shortcomings. First, the rf discharge burning in these gases may involve deposition of fluorine–carbon polymers on the samples under processing, the electrodes and walls of the discharge chamber (a layer of sulfur is deposited in the case of SF_6), and it is necessary to add oxygen into the discharge volume to prevent this undesirable process. Second, these gases live long in the Earth's atmosphere and may destroy the ozone layer, and also contribute to the so-called 'greenhouse effect' [6]. The dissociation degree of these gases in technological chambers is not large [18], and considerable amounts of a gas not used during a technological process are transported via vacuum pumps into the atmosphere. Therefore NF_3 may present a more promising alternative to these gases. The discharges in NF_3 do not form polymer layers, and the lifetime of NF_3 molecules in atmosphere is comparatively small [6]. We will show below that NF_3 also possesses an additional advantage in the form of almost complete dissociation of NF_3 molecules under discharge conditions usually employed in technological processes. Fluorine atoms made free in considerable number lead to the enhanced rate of etching materials under processing. Therefore it is of considerable interest to study modes of burning and characteristics of rf discharge in NF_3.

However, the properties of rf capacitive discharge in NF_3 remain almost unknown until now. Paper [19] reports a single voltage–power characteristic registered at fixed gas

pressure in the industrial etching system (GIR 100 made by Alcatel). Paper [20] contains the measurements of the impedance and phase shift between rf current and voltage in different NF_3/Ar mixtures in GEC Reference cell. In the same chamber the authors of [14] studied the effect of gas pressure on the power, impedance and phase shift in NF_3 mixtures with argon and some other gases. As we observe, the experiments in [14, 19, 20] were performed in asymmetric technological reactors. Until now the available references do not contain the information on modes of burning and characteristics of the symmetric rf capacitive discharge in NF_3.

In contrast to NF_3 used for etching, the second gas we studied, SiH_4, is widely applied for depositing hydrogenated amorphous and microcrystalline silicon and silicon nitride [21–30]. It induced the appearance of numerous experimental and theoretical papers devoted to studying the properties of rf discharge in this gas (see, i.e. [31–40]).

As is known [41–49], the rf capacitive discharge may burn in two different modes: weak-current (α-) and strong-current (γ-) ones. The weak-current mode is characterized by low conductance of near-electrode sheaths, the ionization being accomplished by electrons gaining energy in the rf electric field within the plasma volume [41–43]. However, having applied fluid modelling, the authors of paper [44] demonstrated that in α-mode cold electrons acquired the energy necessary for ionization when the near-electrode sheath expanding in the cathode phase swept them into the plasma volume. The authors of paper [44] called α-mode a 'wave riding mode'. Under transition to the strong-current mode electron avalanches develop within near-electrode sheaths, the ionization occurs primarily near the sheath boundaries and the sheath conductance increases abruptly.

As described in papers [31, 33], rf capacitive discharge in SiH_4 also possesses two modes of burning. With the silane pressure fixed, on increasing rf voltage the discharge experiences a transition from the weak-current α-mode to another mode, a more resistive one, which the authors of papers [31, 33] presented as γ-mode. This transition is accompanied with an abrupt increase of the deposition rate of the a-Si : H film [31], as well as the intense formation of dust particles in the discharge volume [33]. However, Boeuf and Belenguer [34] showed with the numerical simulation that the transition observed is not a transition to the strong-current γ-mode but is induced by an abrupt increase of electron losses. The authors of [34] made an assumption that the attachment of electrons to dust particles formed increases the loss of electrons. This involves the increase of the rf field in the plasma volume and the growth of delivered power. Later this resistive mode was denoted as γ' [36].

In paper [49] it was shown that rf discharge in SF_6 might burn not only in the weak-current α- and strong-current γ-modes but also in the so-called dissociative δ-mode. This δ-mode is characterized by a high degree of SF_6 dissociation, high plasma density, electron temperature and active discharge current, and it is intermediate between the α- and the γ-modes. The δ-mode appears due to a sharp increase in the dissociation rate of SF_6 molecules via electron impact starting after a certain threshold value of rf voltage, when a sufficient number of high energy electrons capable of dissociating SF_6 molecules appear in the discharge. At the same time the threshold

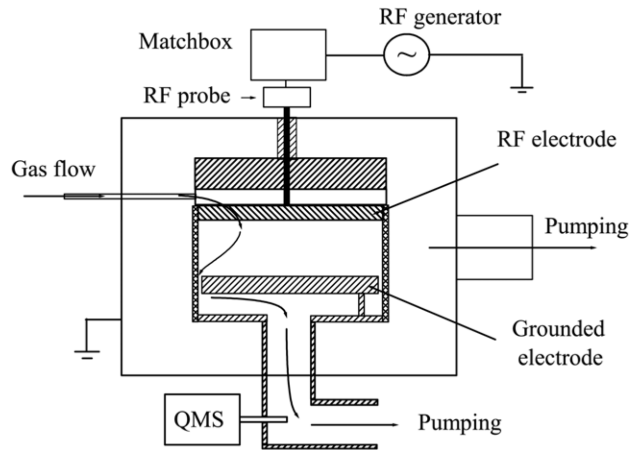

Figure 1. Schematic of our experimental set-up.

ionization energy of SF_x (x = 1–5) radicals formed is below the ionization potential of SF_6 molecules. The discharge transition from the weak-current α–mode to the δ-mode is not accompanied by the breakdown of the near-electrode sheaths but by the appearance of the flow of high energy electrons out of the sheath.

The aim of the present paper is to clarify whether the δ-mode can exist in other gases or it is inherent only to SF_6. This paper shows that the dissociative δ-mode is clearly manifested in NF_3 and SiH_4. The current–voltage characteristic (CVC) of the discharge in NF_3 at the pressures $p > 0.07$ Torr possesses the S-like shape, where the lower part of the CVC relates to the weak-current α-mode, which then transforms to the dissociative δ-mode. At lower NF_3 pressure we observe only the δ-mode. During the transition from the α- to the δ-mode the discharge becomes more resistive; we observe the intense dissociation of gas molecules via electron impact up to the complete decay of NF_3 molecules. The CVC of the discharge in SiH_4 assumes the S-like shape at the pressures $p > 1$ Torr. The dissociation degree of SiH_4 molecules in the δ-mode may attain 70%. The reaction products formed possess much lower ionization potentials, and they serve as an easily ionized admixture to the basic gas leading to an abrupt increase of the discharge current.

2. Description of the experiment

In our research device (see figure 1) the capacitive rf discharge was ignited at the frequency of rf field $f = 13.56$ MHz, and a number of measurements were performed for $f = 27.12$ MHz. The experiments were conducted with NF_3 and SiH_4 within the gas pressure range $p \approx 0.015$–1.5 Torr with the inter-electrode gap values of $d = 25$, 20.4 and 15 mm. Parallel-plate aluminium electrodes had a diameter of 143 mm. The rf voltage with the amplitude $U_{rf} < 1000$ V from the generator was fed through the matchbox to the potential electrode while another electrode was grounded. Electrodes were located inside the fused silica tube with an inner diameter of 145 mm. The gas under study was fed into the inner chamber through small orifices in one electrode and then pumped out through the gap between the second electrode and the wall of the fused silica tube. This discharge chamber was completely

surrounded with a grounded grid and put inside a large grounded chamber with a diameter of 315 mm and a height of 231 mm (see figure 1). The grounded grid, the fused silica tube around the electrodes and a lower gas pressure (by 1–2 orders of magnitude) in the large chamber prevented the ignition of the self-sustained rf discharge in it. The outer chamber possessed a sufficiently large window of fused silica enabling one to observe the discharge behaviour in the process of cleaning the inner chamber.

Rf voltage U_{rf} was measured with the rf voltage–current probe (rf probe Z'SCAN, Advanced Energy). This rf probe was located at the minimum possible distance from the rf electrode. Z'SCAN permitted to register not only the values of rf voltage, rf current, phase shift angle φ between current and voltage and delivered power for the basic frequency but also the values of rf current and voltage for harmonics. We used the rf generator RF5S (RF Power Products Inc.) with the maximum delivered power of 500 W and the matching box PFM (Huettinger Elektronik GmbH) of L-type. In a number of experiments a more powerful rf generator (up to 2000 W) (Advanced Energy) was also used.

Gas pressure was monitored with 10 and 1000 Torr capacitive manometers (MKS Instruments). The gas flow was set with a mass flow controller to 5 sccm (sccm denotes standard cubic centimetre per minute), and the pressure was regulated by throttling the outlet to the pump. The adaptive pressure controller supported the constant value of the gas pressure (in those cases when it was kept constant in the process of measurements).

The quadruple mass-spectrometer QMS 421 (Balzers) analysed the content of the neutral gas leaving the discharge chamber. The gas under analysis was fed from the system of the chamber pumping out through a narrow capillary, which permitted to perform gas analysis up to pressures of the order of 1 Torr.

3. Rf discharge in NF_3

3.1. Experimental results

First let us present the main results we obtained for NF_3. Figure 2 depicts the Ohmic rf current (CVC) for NF_3 pressure $p = 0.375$ Torr against rf voltage applied (see also CVCs, the phase shift between rf current and voltage and active power in figure 3 for different NF_3 pressure). It is clear from the figures that at NF_3 pressures exceeding 0.07 Torr the CVC of the rf discharge possesses an S-like shape. The lower branch starting from the discharge extinction voltage U_{ext} represents a weak-current mode with a characteristic value of the discharge current about 100–200 mA. Then, after the rf voltage attains some threshold value $U_{\alpha-\delta}$, the discharge current and active rf power begin to increase fast with simultaneous decrease of the rf voltage across the electrodes, the discharge experiences a transition to the dissociative δ-mode. With the increase in the discharge current the weak luminosity of the discharge characteristic of the α-mode grows abruptly after the transition to the δ-mode. On increasing the discharge current further the rf voltage across the electrodes approaches its minimum value $U_{\delta.\min}$, and we embark on the upper branch of the CVC. Here with the increase in the rf voltage the discharge current first attains its maximum value and then decreases

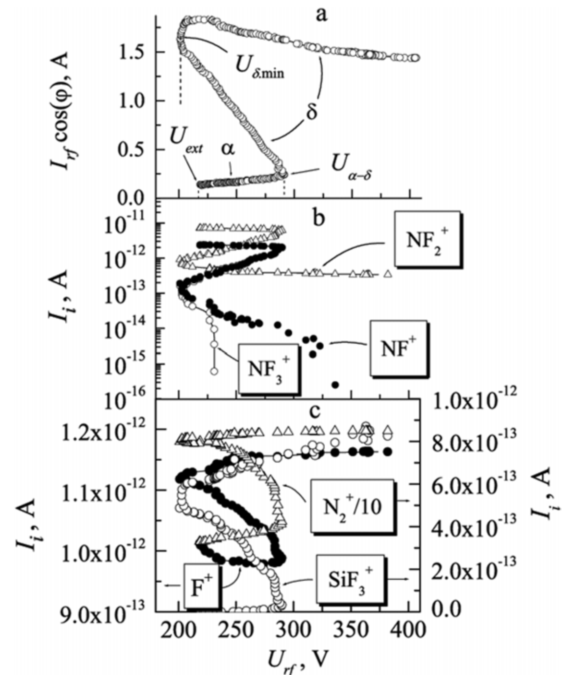

Figure 2. Ohmic rf current (a), NF_3^+, NF_2^+ and NF^+ peak intensities (b), as well as N_2^+, SiF_3^+ and F^+ peak intensities (c) against the applied rf voltage for the inter-electrode gap of $L = 25$ mm and NF_3 pressure of $p = 0.375$ Torr.

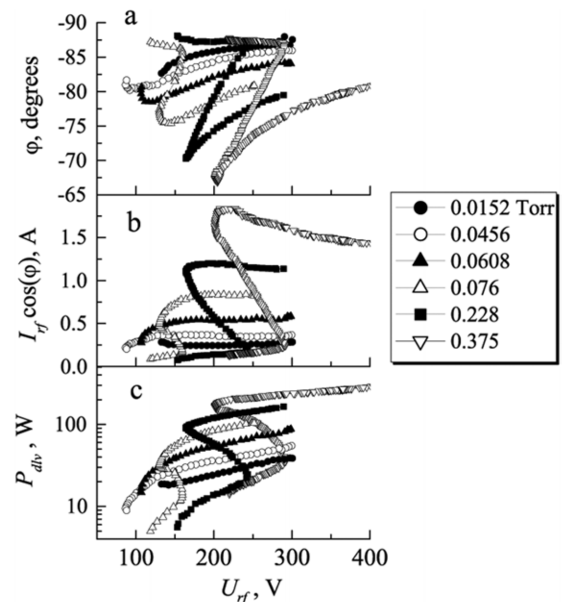

Figure 3. Phase shift angle between rf current and voltage (a), Ohmic rf current (b) and active power (c) against applied rf voltage. NF_3, $L = 25$ mm.

slowly. Figure 3 shows clearly that the phase shift is much larger in the δ-mode than one in the α-mode, therefore the δ-mode is more resistive. It also follows from figure 3 that in an established δ-mode (the upper part of CVC) the phase shift φ behaviour is similar to the one in the α-mode of the rf discharge in electro-positive gases (argon, nitrogen [46]) and in oxygen [47]. That is, the growth of the rf voltage is accompanied by the decrease in the phase shift angle. In the case of a burning discharge in the α-mode, when the

concentration (consequently, the conductivity) of the quasi-neutral plasma is large, the rf current is limited by the capacitive impedance of near-electrode sheaths, which depends on their thickness d_{sh}. On increasing the plasma concentration the thickness of the sheaths d_{sh} and their capacitive impedance vary comparatively weakly, whereas the Ohmic resistance of the quasi-neutral plasma diminishes considerably. Therefore with the rf voltage increasing the phase shift angle decreases tending to the value-$\pi/2$, and the discharge becomes more capacitive in nature. Correspondingly, the Ohmic current $I_{rf}\cos(\varphi)$ also decreases what we observe in figures 2 and 3.

It may be assumed from the curves presented in figure 3, that at low pressure ($p < 0.06$ Torr) the discharge CVC is the upper branch of the S-like characteristic, i.e. only a dissociative mode exists under these conditions. This conclusion is supported by the absence of the NF_3^+ peak in the mass-spectrum at low NF_3 pressure.

In figure 2, apart from the CVC $I_{rf}\cos(\varphi)$, we present the intensities of the peaks NF_3^+, NF_2^+, NF^+, N_2^+, SiF_3^+ and F^+ against the applied rf voltage registered at the NF_3 pressure $p = 0.375$ Torr. It follows from the figure that the dissociation degree of the gas is small in the weak-current α-mode, and mainly NF_3, NF_2, NF and N_2 molecules as well as atomic fluorine F leave the discharge volume. The mass-spectrum also contains a weak SiF_3^+ peak indicating the presence of a volatile product of etching silicon, SiF_4. This peak appeared because fluorine atoms had etched the surface of the silicon tube of our discharge chamber, other possible sources of silicon (semiconductor plates, specimen, silicon-containing impurities on the electrodes) were absent in this case. However, when the rf voltage attained the value $U_{\alpha-\delta}$, the discharge experienced a transition to the δ-mode, the intensities of the NF_3^+, NF_2^+, NF^+ peaks decreased abruptly whereas the intensities of the N_2^+, F^+ and SiF_3^+ peaks increased. Under conditions of the CVC upper branch in the δ-mode first the NF_3^+ peak disappeared at the rf voltage of 230 V, and then at 350 V the NF^+ peak followed suit, i.e. we observe the complete dissociation of NF_3 molecules in our discharge. At the rf voltage of 380 V the gas mixture leaving the discharge gap contains 79% of molecular nitrogen, 11% of atomic fluorine, 7% of SiF_4 and 3% of NF_2. The content of the gas mixture within the discharge gap remains almost constant under conditions of the CVC upper branch with the rf voltage growing. At actually constant N_2 and F concentrations we observe a weak growth of the SiF_4 concentration and a small decrease in the NF_2 concentration. Probably, at higher rf voltage we can also attain a complete decay of the NF_2 molecules.

Note that the data on the gas mixture content are only approximate. A capillary gathering gas tests for mass-spectrometric analysis was located outside the discharge chamber downstream. The F atoms formed in the discharge volume can react with aluminium electrodes (producing a layer of AlF_3 on them), with the surface of the fused silica tube (what we observe as the SiF_3^+ peaks indicating the presence of the volatile product of etching, SiF_4), with the walls of the vacuum chamber and the capillary. The main portion of the atomic fluorine recombines, perhaps, at the capillary walls forming fluorine molecules. Therefore the concentration value of the atomic fluorine obtained with the mass-spectrometer is clearly understated.

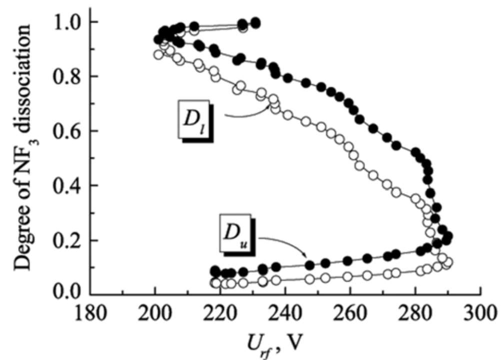

Figure 4. Dissociation degrees D_l and D_u of NF_3 molecules against applied rf voltage for the inter-electrode gap $L = 25$ mm and NF_3 pressure $p = 0.375$ Torr.

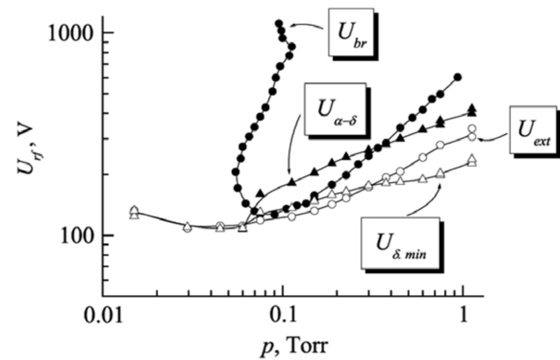

Figure 5. Breakdown curve U_{br}, extinction curve U_{ext}, transition curve from α- to δ-mode $U_{\alpha-\delta}$ and the curve with the smallest rf voltage across the electrodes in δ-mode $U_{\delta.min}$ in NF_3 with $L = 25$ mm.

Figure 4 shows the dissociation degrees D_u and D_l of NF_3 molecules calculated according to the formulae [50]:

$$D_u = \frac{I_0(NF_3^+) - I_{pl}(NF_3^+)}{I_0(NF_3^+)}, \quad (1)$$

$$D_l = \frac{I_0(NF_3^+) - I_{pl}(NF_3^+)}{I_0(NF_3^+) + I_{pl}(NF_3^+)}, \quad (2)$$

where I_0 and I_{pl} are the intensities of NF_3^+ peaks without the rf discharge and with it, respectively. The true value of dissociation degree of NF_3 molecules lies between those for D_u and D_l. It follows from the figure that in the α-mode the dissociation degree is approximately equal to 4–10%, after the rf voltage attains the $U_{\alpha-\delta}$ value it increases abruptly, and after getting to the upper CVC branch with the δ-mode the dissociation degree of NF_3 molecules approaches 100%.

Figure 5 shows the breakdown curve U_{br} (rf discharge ignition voltage), the extinction curve U_{ext}, the transition curve from α- to δ-mode $U_{\alpha-\delta}$ and the curve with the smallest rf voltage across the electrodes in the δ-mode $U_{\delta.min}$ in NF_3. The rf breakdown curve in NF_3 similar to ones in other gases possesses a region of multi-valued dependence of rf breakdown voltage on gas pressure in the low-pressure range (to the left of the minimum). The weak-current α-mode may exist only within the range between the discharge extinction curve U_{ext} and the transition curve from α- to δ-mode $U_{\alpha-\delta}$. At the pressure of 0.06 Torr these two curves meet. It is observed

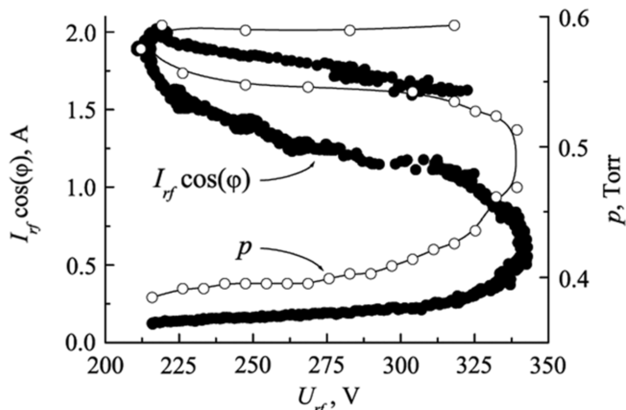

Figure 6. Ohmic rf current and NF_3 gas pressure against applied rf voltage for the inter-electrode gap $L = 25$ mm and initial NF_3 pressure $p = 0.375$ Torr.

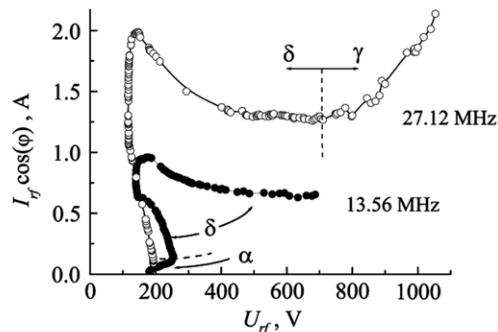

Figure 7. Ohmic rf current against applied rf voltage for the inter-electrode gap $L = 20.4$ mm for the frequency values of $f = 13.56$ MHz and $f = 27.12$ MHz and NF_3 pressure $p = 0.375$ Torr.

from the figure, that at gas pressure below 0.06 Torr the rf discharge burns in the δ-mode within the total range of rf voltage we studied whereas the weak-current α-mode appears only at higher gas pressure. In this figure the extinction curve U_{ext} shows the value of the rf voltage at which the discharge is extinguished. As we observe, in the pressure range above 0.3 Torr the discharge extinction occurs at the rf voltage exceeding the smallest rf voltage across the electrodes in the δ-mode $U_{\delta.min}$, and the curve $U_{\delta.min}$ runs below the extinction curve of the rf discharge U_{ext}.

Since the intense dissociation of gas molecules via electron impact takes place in the δ-mode, the total number of molecules in the discharge volume increases. In the process of registering the results presented above our automatic vacuum valve kept the gas pressure constant increasing the gas pumping rate when the number of molecules increased. Let us now observe the variations of the discharge CVC and gas pressure when the vacuum valve keeps constant the pumping rate rather than the gas pressure. We feed NF_3 into the chamber with the rate of 5 $cm^3\,min^{-1}$, fix the pumping rate constant with a valve establishing the initial gas pressure at 0.375 Torr (0.5 mbar), and then ignite the discharge. The results of measurements are presented in figure 6. The CVC clearly retained its S-like shape. In the weak-current α-mode with rf voltage growing the gas pressure increases slowly, but on approaching the rf voltage of the $\alpha - \delta$ transition, $U_{\alpha-\delta}$, the pressure growth rate increases. After attaining $U_{\alpha-\delta}$, the discharge experiences a transition to the δ-mode, the growth of the Ohmic current $I_{rf}\cos\varphi$ being accompanied by the decrease of the rf voltage across the electrodes and the fast growth of the gas pressure. After the Ohmic current attained its maximum value and the CVC came to the upper part of the S-like characteristic the gas pressure is stabilized practically. On increasing the rf power (and the rf voltage) the small growth of the gas pressure is associated with the increase in the number of molecules due to dissociation of reaction products NF_x ($x = 1, 2$), as well as to the heating of the neutral gas. The weak variation of the gas pressure at this section of the CVC indicates the cessation of the fast dissociation of gas molecules.

In a number of cases we performed the measurements not only for the frequency $f = 13.56$ MHz, but also for $f = 27.12$ MHz. Figure 7 shows the CVCs for NF_3 pressure value $p = 0.375$ Torr and the inter-electrode gap $L = 20.4$ mm. CVC for $f = 13.56$ MHz possesses a section with the weak-current α-mode, as well as two branches with the δ-mode. Because of the limited power of the rf generator we could not achieve the strong-current γ-mode in this case. The CVC for $f = 27.12$ MHz does not contain a section with the weak-current α-mode, the CVC starts at once with the dissociative δ-mode, and at sufficiently high rf voltage the strong-current γ-mode also appears. The value of the Ohmic current for $f = 27.12$ MHz exceeds one for $f = 13.56$ MHz almost twice. Perhaps the weak-current α-mode may appear in the CVC for $f = 27.12$ MHz at higher NF_3 pressure.

3.2. Discussion

Thus let us consider what processes in NF_3 may produce the phenomena described above. For thermo dissociation of NF_3 molecules the gas has to be heated only to 400 °C [18]. For comparison let us point out that the dissociation of SF_6 and CF_4 molecules occurs at the temperatures of 800 °C and 1400 °C, respectively. The NF_3 molecules may decay as a result of the dissociative attachment of electrons

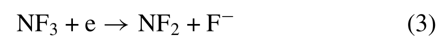

$$NF_3 + e \rightarrow NF_2 + F^- \qquad (3)$$

with the threshold energy for it approximately equalling zero because the energy of electron affinity to a fluorine atom (3.6 eV) exceeds the NF_2–F bond energy (2.5 eV) [51]. The threshold energy for dissociating CF_4 molecules via electron impact is equal to 12.6 eV.

The NF_3 and its radicals possess the following bond dissociation energies: NF_2–F, 2.5 eV [51] (3.2 eV [52], 2.6 eV [53]), NF–F, 2.7 eV [52] (2.5 eV [53]), N–F, 2.6 eV [54]. However, the probability of direct splitting the NF_3 molecules with the energy, say, 4 eV, is very small because of the short-time electron–molecule interaction during which heavy atoms (radicals) have no time to get the momentum required for flying off. The dissociation of molecules has a two-stage pattern and it is accomplished via excitation of electronic or electronic-vibration states of the molecule with a subsequent decay of the excited molecule into atoms [55]. In the case of NF_3 the dissociation process goes according to the scheme

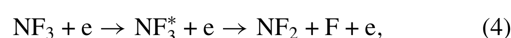

$$NF_3 + e \rightarrow NF_3^* + e \rightarrow NF_2 + F + e, \qquad (4)$$

where the NF_3^* symbol denotes the ^{3}E (triplet) or ^{1}E (singlet) electronically excited states with the threshold energy of 8.3 eV (for the ^{3}E state) [56].

The process of ionizing NF_3 molecules and radicals via electron impact may proceed as follows:

$$NF_3 + e \rightarrow NF_3^+ + 2e, \quad (5)$$

$$NF_3 + e \rightarrow NF_2^+ + F + 2e, \quad (6)$$

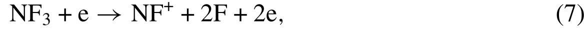

$$NF_3 + e \rightarrow NF^+ + 2F + 2e, \quad (7)$$

$$NF_2 + e \rightarrow NF_2^+ + 2e, \quad (8)$$

$$NF + e \rightarrow NF^+ + 2e, \quad (9)$$

at the same time, for these reactions to occur the following energy is required: (5)—13.2 eV [54], (6)—14.6 eV [57], (7)—17.9 eV [54], (8)—11.4 eV [57], (9)—12.0 eV [52]. Thus the ionization potential for NF_2 and NF radicals (11.4 eV and 12.0 eV, respectively) is remarkably lower than the ionization potential of NF_3 molecules (13.2 eV). Similar to the case of SF_6 molecules presented in [49], the NF_2 and NF radicals formed under NF_3 dissociation play the role of an easily ionized admixture.

As is known [58–60], lowering gas pressure involves the growth of the electron temperature T_e. Probably, at low pressure ($p < 0.06$ Torr) in the rf discharge in NF_3 the electron temperature T_e is comparable with the threshold dissociation energy of 8.3 eV. Therefore just after the ignition the rf discharge burns in the dissociative δ-mode, because the energy of electrons is sufficiently high to allow for the reactions of dissociating NF_3 molecules.

Regrettably we had no opportunity to perform probe measurements of the electron temperature in the rf discharge in NF_3. Similar data are also absent in the papers of other authors. However we know that in a strongly electro-negative gas SF_6 $T_e \approx 6$–8 eV [49, 61]. The electron temperature in NF_3 would have also be high. The cross-section of dissociative attachment to NF_3 molecules (process (3)) possesses a maximum at the electron energy of $\varepsilon \approx 1.8$ eV and it tends to zero at $\varepsilon \approx 4$ eV [62]. Therefore the electrons having the energy $\varepsilon \leqslant 4$ eV are lost due to attachment forming negative F^- ions as a result. Perhaps the electron temperature in NF_3 has to exceed remarkably (by some eV) the value of 4 eV in order to compensate this loss of free electrons and to provide the ionization rate required for discharge sustainment and rf current transport.

With the pressure growing the electron temperature becomes lower and the conditions appear for the existence of the weak-current α-mode of the rf discharge. At the smallest voltage for burning (before the extinction) the electron temperature is usually at maximum (at the gas pressure fixed), and increasing rf voltage in the weak-current mode induces the decrease in T_e [46, 47]. This explains why in figure 2 the concentration of fluorine atoms increases before the discharge extinction (a moderate increase of the dissociation degree of NF_3 molecules can also be observed in figure 4). While, starting from some gas pressure, the electron temperature in the α-mode becomes insufficiently high to dissociate NF_3 molecules and radicals, the dissociative attachment of electrons (3) determines in considerable degree (and limits) the dissociation degree of gas molecules under these conditions. The matter is that a free electron attached to a fluorine atom loses its ability to acquire energy in the rf electric field and to produce the dissociation of gas molecules. A negative fluorine atom F^- will remain in the quasi-neutral plasma until it recombines with a positive ion or until a free electron with the energy above 3.6 eV collides with it and removes the attached electron off it. All free electrons cannot be trapped by fluorine atoms, because just free electrons must perform the ionization of gas molecules and the rf current transport through the plasma volume. Therefore in the weak-current α-mode the dissociation degree of NF_3 molecules is not high and it grows uniformly with the rf voltage increasing due to the plasma density growth. However, as was shown with probe technique in [49] for SF_6, with the growth of the rf voltage the energy and concentration of high energy electrons from the 'tail' of the electron energy probability function (EEPF) in the quasi-neutral plasma also grow. At low electron temperature just fast electrons from the EEPF 'tail' colliding with molecules may induce their dissociation. Perhaps when the rf voltage approaches a certain threshold value $U_{\alpha-\delta}$, the concentration of high energy electrons becomes sufficiently high for the start of a fast dissociation of NF_3 molecules and NF_2 and NF radicals. Owing to low ionization potentials of NF_2 and NF radicals, the ionization rate and plasma density in the discharge increase abruptly. In the dissociation processes the free fluorine atoms are also produced that trap free electrons with low energy, and the concentration of negative F^- ions grows in the plasma. In order to provide the ionization rate of gas molecules via electron impact sufficient for discharge sustainment and rf current transport, the rf electric field in the plasma volume increases [59]. This in its turn increases the concentration of high energy electrons as well as the temperature of cold electrons, and the dissociation of gas molecules is accelerated. The increase of the plasma density together with the simultaneous accumulation of negative F^- ions leads to the increase in the discharge resistivity and a considerable growth of the current.

Note that when the rf voltage achieves the value $U_{\alpha-\delta}$ the discharge transition from $U_{\alpha-\delta}$ to $U_{\delta.\min}$ in figure 2 occurs by itself after reaching manually the threshold value, without changing the rf generator tuning. The emf E_{rf} of the rf generator remains constant during this transition; the resistance Ω of the external circuit also does not change. Therefore, according to the Ohm's law for the closed circuit, because of the fast growth of the rf current I_{rf} the rf voltage across the electrodes U_{rf}

$$U_{rf} = E_{rf} - I_{rf} \cdot \Omega \quad (10)$$

decreases with the fixed E_{rf} and Ω. We can see from figure 2 that during the transition from $U_{\alpha-\delta}$ to $U_{\delta.\min}$ the decrease in the rf voltage across the electrodes is accompanied by the linear growth of the current. It is especially evident at higher pressure $p > 0.5$ Torr. Under these conditions the transition takes place in a jump during which the rf probe Z'SCAN has time to register only several points (with the possible rate of measurement up to 30 points per second).

Consideration of our experimental data reveals that the NF_3 discharge transition from α- to δ-mode occurs when the ratio of the delivered power to gas pressure approaches a critical value $P_{dlv}/p = 55 \pm 15$ W Torr^{-1}. At the same time, the power per unit area of the electrode S is equal to

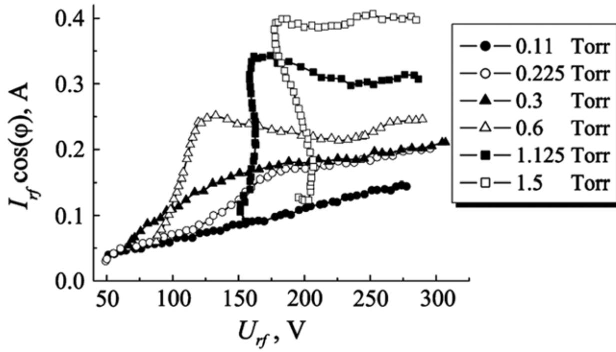

Figure 8. Ohmic rf current against applied rf voltage. SiH_4, inter-electrode gap $L = 15$ mm.

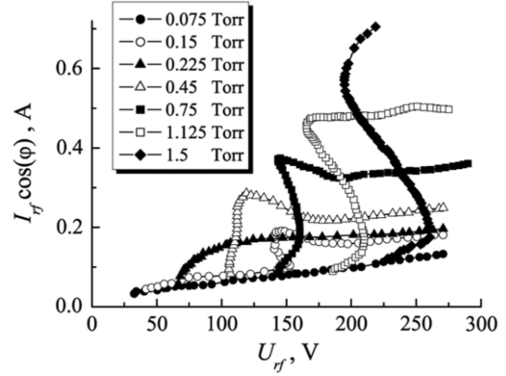

Figure 9. Ohmic rf current against applied rf voltage. SiH_4, inter-electrode gap $L = 25$ mm.

$P_{\mathrm{dlv}}/pS = 0.34 \pm 0.09\,\mathrm{W\,cm^{-2}\,Torr^{-1}}$, the rf Ohmic current equals $I_{\mathrm{rf}}\cos\varphi = 0.175 \pm 0.025$ A, and the current density is $j_{\mathrm{rf}} = 1.1 \pm 0.16\,\mathrm{mA\,cm^{-2}}$.

Thus, it is expedient to consider three different modes of the rf capacitive discharge in NF_3: a weak-current α-mode, a dissociative δ-mode and a strong-current γ-mode. In the weak-current α-mode the ionization of gas molecules is accomplished by electrons swept out of the near-electrode sheath by its moving boundary [44]. In the dissociative δ-mode the dissociation of gas molecules and the subsequent ionization of the radicals formed is accomplished by the electrons having acquired their energy due to Joule heating in the rf electric field in the plasma volume. In the strong-current γ-mode the electron avalanches developing within the near-electrode sheaths dominate as a source of charged particles.

4. Rf discharge in SiH_4

Now consider the characteristics of the rf discharge in silane. In this gas the dissociative δ-mode also happened to be clearly expressed. Figure 8 shows CVCs in SiH_4 for the inter-electrode gap $L = 15$ mm. At the smallest silane pressure $p = 0.11$ Torr presented in the figure we observe the weak-current α-mode within the total range of rf voltage studied in this case. At higher pressure $p = 0.225$ Torr with the increase of the rf voltage first the discharge is burning in the weak-current mode, but at $U_{\mathrm{rf}} > 120$ V there occurs a transition to the dissociative δ-mode, which is more resistive (in the α-mode the phase shift angle is $\varphi \approx -87^{\circ}$, whereas in the δ-mode φ approaches -80°). This leads to the increase in the Ohmic current of the discharge. At higher pressure the weak-current mode is observed only before the discharge extinction. Starting from the pressure value about 1 Torr, the CVC assumes the S-like shape (similar to the case with NF_3 described above). We observe similar CVCs in figure 9 for the inter-electrode gap of 25 mm, but in this case the CVCs assume the S-like shape starting from the pressure value about 0.5 Torr.

In figure 10 we present the intensities of the H_2^+ and SiH_4^+ peaks, we registered downstream. With the rf voltage growing the concentration of hydrogen molecules increases fast whereas the SiH_4 concentration decreases. Figure 11 depicts the CVCs and the dissociation degrees D_{l} and D_{u} of SiH_4 molecules determined according to formulas (1) and (2) (inserting SiH_4^+ in them instead of NF_3^+). In the α-mode (the

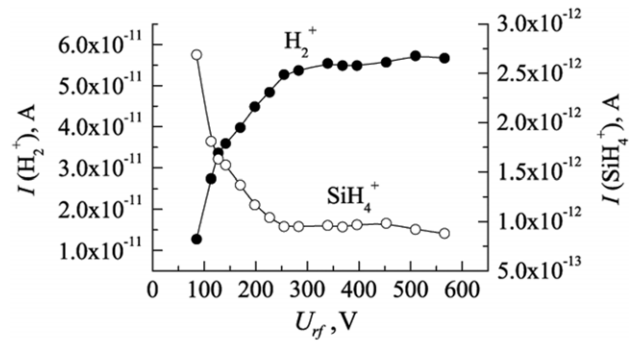

Figure 10. SiH_4^+ and H_2^+ peak intensities against applied rf voltage for the inter-electrode gap $L = 25$ mm and SiH_4 pressure $p = 0.375$ Torr.

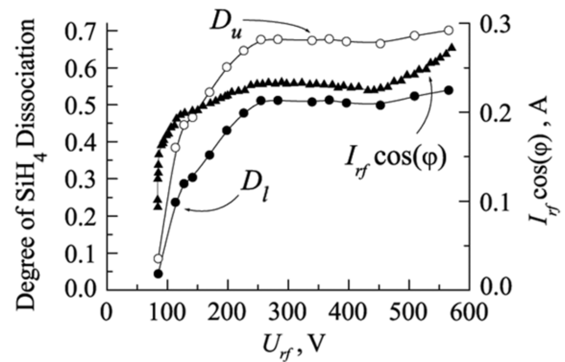

Figure 11. Ohmic rf current and dissociation degrees D_{l} and D_{u} of SiH_4 molecules against applied rf voltage for the inter-electrode gap $L = 25$ mm and pressure $p = 0.375$ Torr.

smallest rf voltage, $U_{\mathrm{rf}} = 85$ V) the dissociation degree of SiH_4 molecules does not exceed 10%. At this SiH_4 pressure ($p = 0.375$ Torr) at the initial section of the CVC (near the discharge extinction) the growth of the Ohmic discharge current and the transition from α- to δ-mode occur at almost constant rf voltage, the dissociation degree of SiH_4 molecules increasing fast. Then the growth of the discharge current is accompanied by the rf voltage increase, and in the δ-mode the dissociation degree may attain 50–70%. The high dissociation degree of SiH_4 molecules (from 35% to 70%) were also obtained by the authors of [39] in agreement with our results. At the rf voltage values from $U_{\mathrm{rf}} = 220$ V to

$U_{rf} = 440$ V the Ohmic discharge current and dissociation degree of SiH_4 molecules remain practically unchanged with the growth of U_{rf}. At $U_{rf} = 440$ V we observe the fast growth of the discharge current, the dissociation degree of SiH_4 also increasing. Perhaps the transition from the δ- to γ-mode takes place at this rf voltage. It is accompanied by a considerable increase of the plasma luminosity at the boundaries of the near-electrode sheaths.

Note that the actual degree of SiH_4 dissociation in the discharge volume may differ from the one we registered. We evaluate the dissociation degree from the SiH_4^+ peak intensity analysing the tests of the gas mixture taken downstream. However the SiH_4 molecules may be lost in the discharge not only because of the dissociation process but also due to a number of chemical reactions [35, 37, 38], e.g.:

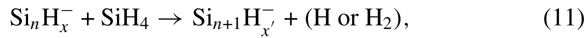

$$Si_nH_x^- + SiH_4 \rightarrow Si_{n+1}H_{x'}^- + (H \text{ or } H_2), \quad (11)$$

$$SiH_4 + SiH_2 \rightarrow Si_2H_6, \quad (12)$$

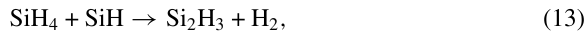

$$SiH_4 + SiH \rightarrow Si_2H_3 + H_2, \quad (13)$$

$$SiH_4 + Si \rightarrow Si_2H_2 + H_2, \quad (14)$$

$$SiH_4 + H \rightarrow SiH_3 + H_2, \quad (15)$$

$$SiH_4 + Si_2H_4 \rightarrow Si_3H_8. \quad (16)$$

Therefore, in this case it is more expedient to use the term 'the silane fractional depletion' [39].

The dissociation of SiH_4 molecules via electron impact may occur as follows [38]:

$$SiH_4 + e \rightarrow SiH_3 + H + e, \quad (17)$$

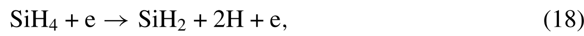

$$SiH_4 + e \rightarrow SiH_2 + 2H + e, \quad (18)$$

where the probability of reactions (17) and (18) is 17% and 83%, respectively. For the dissociation reactions (17) and (18) to take place the electrons with the threshold energy of 8.4 eV are required [63]. Similar to the case with NF_3 described above, the ionization potential of SiH_4 molecules (11.65 eV) exceeds considerably the ionization potentials of the radicals SiH_3 (8.14 eV), SiH_2 (8.92 eV) and SiH (7.89 eV) [64], i.e. the reaction products formed as a result of dissociation are an easily ionized admixture to SiH_4. Besides, the energy required for dissociation is close to the ionization energies of reaction products. Perhaps on attaining the critical value $U_{\alpha-\delta}$ of the rf voltage when a sufficient number of high energy electrons appear in the discharge, an intense dissociation of SiH_4 molecules and a subsequent ionization of easily ionized reaction products produce a fast growth of the discharge current and a transition to the dissociative δ-mode. Negative ions (SiH_3^- and SiH_2^-) also play an important role, not only leading to the increase of the rf electric field in the plasma volume [65], but also enhancing a growth of dust particles [36, 37] (e.g. due to reaction (11)).

Now let us check whether the near-electrode sheaths are broken down in the dissociative δ-mode. As we have shown earlier in [48], the time of electron motion through a near-electrode sheath is small compared with the period T, therefore the breakdown of the sheath with a nonuniform distribution of the rf electric field inside it $E(x)$ may be described with the breakdown criterion in the dc electric field

$$\gamma \left[\exp\left(\int_0^{d_{sh}} \alpha \, dx \right) - 1 \right] \equiv M = 1, \quad (19)$$

where γ is the ion–electron emission coefficient from the electrode surface. We will assume the rf electric field E to drop linearly on the way from the electrode surface to the sheath boundary:

$$E(x) = \frac{2U_{sh}}{d_{sh}} \left(1 - \frac{x}{d_{sh}} \right), \quad (20)$$

where U_{sh} is the maximum rf voltage drop across the near-electrode sheath, d_{sh} is the sheath thickness. We put the origin of coordinates ($x = 0$) at the electrode surface. We neglect the rf voltage drop across the quasi-neutral plasma, and assume that all rf voltage is concentrated within the near-electrode sheaths ($U_{sh} \approx U_{rf}$). The first Townsend coefficient α is written in the form

$$\frac{\alpha}{p} = A \cdot \exp\left(-\frac{Bp}{E(x)} \right) = A \cdot \exp\left(-\frac{Bpd_{sh}}{2U_{rf}(1 - x/d_{sh})} \right), \quad (21)$$

where A and B are constants. Then criterion (19) assumes the form

$$\gamma \left\{ \exp\left[\int_0^{d_{sh}} A \cdot p \cdot \exp\left(-\frac{Bpd_{sh}}{2U_{rf}(1 - x/d_{sh})} \right) dx \right] - 1 \right\} \equiv M = 1. \quad (22)$$

We determine the $\alpha(E/p)$ dependence with the help of the Bolsig code (www.siglo-kinema.com/bolsig.htm), using the cross sections of electron collisions with SiH_4 molecules [66]. In order to perform the calculations according to formulas (19) and (22) we also have to know the coefficient of secondary ion–electron emission (γ). We failed to find in the references either the coefficient γ or the dc breakdown curves in SiH_4 from which this coefficient might be inferred. Therefore we employed for γ determination the CVC we registered and presented in figure 11. It is observed from the figure that the transition from δ- to γ-mode occurs clearly at $U_{rf} = 440$ V . This claim is supported not only by a fast growth of the Ohmic rf current but also by the increase in the plasma luminosity at the boundaries of near-electrode sheaths. The luminosity at the sheath boundaries acquires a characteristic violet tint indicating the appearance of high energy electrons and the development of electron avalanches in the near-electrode sheaths. Perhaps under this transition to the γ-mode one may say that the near-electrode sheath is broken down. If we know the magnitude of the rf voltage corresponding to the δ– γ transition $U_{rf} = 440$ V, gas pressure $p = 0.375$ Torr, as well as the near-electrode sheath thickness $d_{sh} \approx 3.5$ mm, we can determine from formula (22) the value $\gamma = 0.022$ at which the sheath breakdown criterion is met (i.e. $M = 1$). Now let us apply the found value of γ and formula (22) for the conditions of the burning δ-mode ($U_{rf} = 200$ V, $d_{sh} \approx 4$ mm) and find $M = 0.366$, i.e. $M < 1$, therefore the sheath breakdown criterion (22) in the δ-mode is not met. Thus the near-electrode sheaths in the δ-mode are not broken down, i.e. the growth of the Ohmic current takes place not because of the ionization of gas molecules in the near-electrode sheaths (as is the case with the γ-mode), but due to Joule heating in the rf electric field in the plasma volume. It agrees with the conclusion [34], that a more resistive mode of the rf discharge in SiH_4 observed by the authors of [31, 33] is not the γ-mode.

Let us recall that two modes were observed in the rf discharge in SiH_4: on increasing the rf power/pressure the

discharge experiences a transition from the weak-current α-mode to a more resistive one (the authors of [31, 33] thought it to be the strong-current γ-mode). But the authors of [34] have shown that this transition, perhaps, is connected with an abrupt increase in electron losses due to attachment to dust particles formed but not to the transition to the γ-mode. Then this mode began to be called not γ- but γ'-mode [36].

The analysis of data from [31, 33] and the results of our experiments show that, probably, the transition from the α-mode to the γ'-mode is just the $\alpha - \delta$ transition we observe. A natural question arises about the necessity to speak of the δ-mode, as soon as so-called γ'-mode exists. Note that the notation γ' is meant to show the difference between this mode and the γ-mode in which the secondary electrons emitted from the electrodes due to the bombardment with positive ions, dominate in the discharge sustainment. At the same time, the α-mode is the dust free mode, whereas in the γ'-mode the dust particles play an important role in the discharge [36]. However, it is evident that while in the α-mode the dust particles are absent, an additional process has to appear under the transition to the γ'-mode (that did not play a noticeable role in the α-mode), which will lead to dust formation in the discharge volume.

In our opinion, the dissociation of SiH_4 molecules via electron impact ((17) and (18)) is just this process. In favour of this statement we have the following fact: the transition to the δ-mode is accompanied by the appearance of dust particles as well as an abrupt increase of the a-Si : H film deposition rate [31, 33]. As is known [67], for depositing the a-Si : H film the presence of SiH_2 and SiH_3 is required. For the production of these molecules as a result of dissociation reactions (17) and (18), as we said above, the electrons with the threshold energy of 8.4 eV have to be present in the discharge [64]. The neutral and negatively charged SiH_3^- radicals take part in the formation of dust particles [36]. Obviously, the dust particles that are generated and negatively charged lead to enhanced loss of electrons and, as a consequence, to the growth of the rf electric field in the plasma volume and to the increase of the dissociation rate of SiH_4 molecules [36]. But this would already be the consequence of the process whose reason is the 'switching on' of the dissociation of SiH_4 molecules via electron impact at sufficiently high rf voltage. Therefore we suggest calling this mode not a γ'-mode, but a δ-mode. Notation 'γ'' was chosen to show the difference between this mode and the strong-current γ-mode, and it does not carry any information about the processes playing the role in the discharge in this mode. Our choice of the 'δ' letter is not incidental because the Greek counterpart of the word 'dissociation' ('$\delta\iota\alpha\sigma\pi\alpha\sigma\eta$') begins with it.

Besides the γ'-mode is associated with the regime when dust particles appear, and it is inherent only to SiH_4 [36]]. However, we have shown above that the transition of the rf discharge from the α-mode to a more resistive dissociative δ-mode is observed also in NF_3, which neither forms dust particles nor deposits any films but possesses the CVCs that are rather similar to those in SiH_4. The dissociative δ-mode exists in SF_6 and mixtures of SF_6 with oxygen [49], as well as in some other gases (the results will be presented in other our papers), which also do not form dust particles or films. Therefore the dissociative δ-mode is inherent to a number of gases, and the formation of dust particles in SiH_4 as well as the enhanced rate of depositing a-Si : H film [36] are just secondary phenomena, a consequence of the δ-mode burning.

Perhaps negative ions also play a very important role in the onset of the dissociative $\delta-$mode. For example, SF_6^-, SF_5^-, SF_3^-, F_2^-, F^- and O^- ions appear in SF_6 and in the mixtures of SF_6 with oxygen in the processes of dissociation and dissociative attachment [65]. In NF_3 a large amount of fluorine is made free enabling it to form negative F_2^- and F^- ions. In SiH_4 there appear not only negative ions SiH_3^-, SiH_2^- and H^-, but also negatively charged dust particles [36]. Formation of such negative ions/particles increases the resistivity of the discharge [65], and increases the rf electric field in plasma enhancing the dissociation of gas molecules.

The SiH_4 discharge transition from α- to δ-mode occurs when the discharge parameters attain the following threshold values: $P_{dlv}/pS = 0.11 \pm 0.04\,\mathrm{W\,cm^{-2}\,Torr^{-1}}$, $j_{rf} = 0.9 \pm 0.3\,\mathrm{mA\,cm^{-2}}$. These data are in good agreement with those of paper [33] for the transition from α-mode to a more resistive one $P_{dlv}/pS = 0.081\,\mathrm{W\,cm^{-2}\,Torr^{-1}}$, $j_{rf} = 0.6\,\mathrm{mA\,cm^{-2}}$.

5. Conclusions

We have investigated in experiment the rf capacitive discharge in low-pressure NF_3 and SiH_4, registering the CVCs and mass-spectra of the gas leaving the discharge gap. The rf discharge in NF_3 and SiH_4 is shown to exist in three different modes: weak-current α-mode, strong-current γ-mode and dissociative δ-mode, the latter being intermediate between the α- and γ-modes. The dissociative δ-mode is characterized by a high dissociation degree of NF_3 molecules (actually up to 100%) and SiH_4 (up to 70%) via electron impact and high Ohmic current of the rf discharge. The dissociative mode appears starting with some threshold rf voltage when a sufficient number of high energy electrons are available in the discharge for inducing dissociation of molecules when colliding with them. At the same time, the ionization potentials of the radicals formed are remarkably lower than the ionization potential of molecules, therefore these radicals play the role of an easily ionized admixture.

Acknowledgment

The authors express their gratitude to the UNAXIS France—Displays division, Palaiseau, France, for their financial support and for the equipment used in this study.

References

[1] Bruno G, Capezzuto P, Cicala G and Manodoro P 1994 *J. Vac. Sci. Technol.* A **12** 690

[2] Kastenmeier B E E, Oehrlein G S, Langan J G and Entley W R 2000 *J. Vac. Sci. Technol.* A **18** 2102

[3] Hsueh H-P, McGrath R T, Ji B, Felker B S, Langan J G and Karwacki E J 2001 *J. Vac. Sci. Technol.* B **19** 1346

[4] Li X, Hua X, Ling L, Oehrlein G S, Karwacki E and Ji B 2004 *J. Vac. Sci. Technol.* A **22** 158

[5] Reichardt H, Frenzel A and Schober K 2001 *Microelectron. Eng.* **56** 73

[6] Langan J, Maroulis P and Ridgeway R 1996 *Solid State Technol.* **39** 115

[7] Donnelly V M, Flamm D L, Dautremont-Smith W C and Werder D J 1984 *J. Appl. Phys.* **55** 242
[8] Ishii I and Brandt W W 1986 *J. Electrochem. Soc.* **133** 1240
[9] Nordheden K J and Verdeyen J T 1986 *J. Electrochem. Soc.* **133** 2168
[10] Sellamuthu R, Barkanic J and Jaccodine R 1987 *J. Vac. Sci. Technol.* B **5** 342
[11] Perrin J, Meot J, Siefert J-M and Schmitt J 1990 *Plasma Chem. Plasma Process.* **10** 571
[12] Sidhwa A J, Goh F C, Naseem H A and Brown W D 1993 *J. Vac. Sci. Technol.* A **11** 1156
[13] Konuma M and Bauser E 1993 *J. Appl. Phys.* **74** 62
[14] Langan J G, Beck S E, Felker B S and Rynders S W 1996 *J. Appl. Phys.* **79** 3886
[15] Kastenmeier B E E, Matsuo P J, Oehrlein G S and Langan J G 1998 *J. Vac. Sci. Technol.* A **16** 2047
[16] Lee R-L and Terry F L 1991 *J. Vac. Sci. Technol.* B **9** 2747
[17] Lu H Y and Petrich M A 1992 *J. Vac. Sci. Technol.* A **10** 450
[18] Koike K, Fukuda T, Fujikawa S and Saeda M 1997 *Japan. J. Appl. Phys.* **36** 5724
[19] Andries B, Ravel G and Peccoud L 1989 *J. Vac. Sci. Technol.* A **7** 2774
[20] Entley W R, Langan J G, Felker B S and Sobolewski M A 1999 *J. Appl. Phys.* **86** 4825
[21] Collins R W 1986 *J. Vac. Sci. Technol.* A **4** 514
[22] Mataras D, Cavadias S and Rapakoulias D 1993 *J. Vac. Sci. Technol.* A **11** 664
[23] Srinivasan E and Parsons G N 1997 *J. Appl. Phys.* **81** 2847
[24] Chowdhury A I, Klein T M, Anderson T M and Parsons G N 1998 *J. Vac. Sci. Technol.* A **16** 1852
[25] Leroy O, Gousset G, Alves L L, Perrin J and Jolly J 1998 *Plasma Sources Sci. Technol.* **7** 348
[26] Biebericher A C W, Bezemer J and Weg W F 2000 *Appl. Phys. Lett.* **76** 2002
[27] Hadjadj A, Beorchia A, Boufendi L, Huet S and Roca i Cabarrocas P 2001 *J. Vac. Sci. Technol.* A **19** 124
[28] Viera G, Huet S, Bertran E and Boufendi L 2001 *J. Appl. Phys.* **90** 4272
[29] Chen F F 1995 *Phys. Plasmas* **2** 2164
[30] Amanatides E, Hammad A, Katsia E and Mataras D 2005 *J. Appl. Phys.* **97** 073303
[31] Perrin J, Roca i Cabarrocas P, Allain B and Friedt J-M 1988 *Japan. J. Appl. Phys.* **27** 2041
[32] Makabe T, Tochikubo F and Nishimura M 1990 *Phys. Rev.* A **42** 3674
[33] Bohm Ch and Perrin J 1991 *J. Phys. D: Appl. Phys.* **24** 865
[34] Boeuf J P and Belenguer Ph 1992 *J. Appl. Phys.* **71** 4751
[35] Perrine J 1993 *J. Phys. D: Appl. Phys.* **26** 1662
[36] Fridman A A, Boufendi L, Hbid T, Potapkin B V and Bouchoule A 1996 *J. Appl. Phys.* **79** 1303
[37] Kim D-J and Kim K-S 1997 *Japan. J. Appl. Phys.* **36** 4989
[38] Nienhuis G J, Goedheer W J, Hamers E A G, van Sark W G J H M and Bezemer J 1997 *J. Appl. Phys.* **82** 2060
[39] Sansonnens L, Howling A A and Hollenstein Ch 1998 *Plasma Sources Sci. Technol.* **7** 114
[40] Lyka B, Amanatides E and Mataras D 2006 *Japan. J. Appl. Phys.* **45** 8172
[41] Levitskii S M 1957 *Sov. Phys.—Tech. Phys.* **2** 887
[42] Yatsenko N A 1981 *Sov. Phys.—Tech. Phys.* **26** 678
[43] Godyak V A and Khanneh A S 1986 *IEEE Trans. Plasma Sci.* **PS-14** 112
[44] Belenguer Ph and Boeuf J P 1990 *Phys. Rev.* A **41** 4447
[45] Raizer Yu P, Shneider M N and Yatsenko N A 1995 *Radio-Frequency Capacitive Discharges* (Boca Raton, FL: CRC Press)
[46] Lisovskiy V A 1998 *Tech. Phys.* **43** 526
[47] Lisovskiy V A and Yegorenkov V D 2004 *Vacuum* **74** 19
[48] Lisovskiy V, Booth J-P, Landry K, Douai D, Cassagne V N and Yegorenkov V 2006 *Phys. Plasmas* **13** 103505
[49] Lisovskiy V, Booth J-P, Jolly J, Landry K, Douai D, Cassagne V and Yegorenkov V 2007 *Proc. 28th Int. Conf. on Phenomena in Ionized Gases (Prague, Czech Republic)* p 2051
[50] Foest R, Olthoff J K, Van Brunt R J, Benck E C and Roberts J R 1996 *Phys. Rev.* E **54** 1876
[51] Kastenmeier B E E, Matsuo P J, Oehrlein G S and Langan J G 1998 *J. Vac. Sci. Technol.* A **16** 2047
[52] Reese R M and Dibeler V H 1956 *J. Chem. Phys.* **24** 1175
[53] Donnelly V M, Flamm D L, Dautremont-Smith W C and Werder D J 1984 *J. Appl. Phys.* **55** 242
[54] Loughran E D and Mader Ch 1960 *J. Chem. Phys.* **32** 1578
[55] Raizer Y P 1991 *Gas Discharge Physics* (Berlin: Springer) p 75
[56] Rescigno T N 1995 *Phys. Rev.* A **52** 329
[57] Konuma M and Bauser E 1993 *J. Appl. Phys.* **74** 62
[58] Dilecce G, Capitelli M and De Benedictis S 1991 *J. Appl. Phys.* **69** 121
[59] Surendra M and Graves D B 1991 *Appl. Phys. Lett.* **59** 2091
[60] Godyak V A, Piejak R B and Alexandrovich B M 1992 *Phys. Rev. Lett.* **68** 40
[61] Picard A, Turban G, Grolleau B 1986 *J. Phys. D: Appl. Phys.* **19** 991
[62] Harland P W and Franklin J L 1974 *J. Chem. Phys.* **61** 1621
[63] Sakai Y 2002 *Appl. Surf. Sci.* **192** 327
[64] Ali M A, Kim Y-K, Hwang W, Weinberger N M and Rudd M E 1997 *J. Chem. Phys.* **106** 9602
[65] Kakuta S, Petrovic Z Lj, Tochikubo F and Makabe T 1993 *J. Appl. Phys.* **74** 4923
[66] Kurachi M and Nakamura Y 1989 *J. Phys. D: Appl. Phys.* **22** 107
[67] Grill A 1994 *Cold Plasma in Materials Fabrication* (New York: IEEE Press) p 192